Scientia Chromatographica 2014; 6(2):85-103
Instituto Internacional de Cromatografia
http://dx.doi.org/10.4322/sc.2014.023
ISSN 1984-4433

Synthesis of stationary phases containing pyridine, phenol, aniline and morpholine via click chemistry and their characterization and evaluation in supercritical fluid chromatography

Melissa Dunkle[1,2]
Caroline West[3]
Alberto Pereira[2]
Steven Van der Plas[4]
Annemieke Madder[4]
William Farrell[5]
Eric Lesellier[3]
Frédéric Lynen[1]
Pat Sandra[1,2*]

[1]Pfizer Analytical Research Centre (PARC), UGent, Krijgslaan 281 S4-bis, 9000 Gent, Belgium
[2]Research Institute for Chromatography (RIC), President Kennedypark 26, 8500, Kortrijk, Belgium
[3]Institut de Chimie Organique et Analytique (ICOA), Université d'Orléans, CNRS UMR 6005, BP 6759, rue de Chartres, 45067 Orléans Cedex 2, France
[4]Department of Organic Chemistry, UGent, Krijgslaan 281 S4-bis, B-9000 Gent, Belgium
[5]Pfizer Global Research and Development, La Jolla, 10770 Science Center Drive, San Diego, CA 92121, USA

Received: October 10, 2013
Accepted: December 17, 2013

Abstract

Stationary phases containing pyridine, phenol, aniline and morpholine groups were synthesized using copper (I)-catalyzed azide-alkyne cycloaddition *click* reactions. The backbone of the stationary phases was aminopropyl silica. The stationary phases were evaluated in packed-column supercritical fluid chromatography (pSFC) with acidic and basic solutes without addition of additives. The analysis of metoclopromide and its impurities by SFC-time-of-flight mass spectrometry (SFC-TOFMS) on the phenol phase is presented. In the *click* reaction, the 1,2,3-triazole ring is formed and to assess its influence on the polarity/selectivity, the *click* phases were compared to a commercial available 1,2,4-triazole hydrophilic interaction liquid chromatography (HILIC) phase. The phases were also compared to two extensively used stationary phases in SFC namely 2-ethyl pyridine and bare silica. To allow comparison with other phases used in SFC, linear solvation energy relationships (LSER) of the *click* phases were determined.

Keywords: Packed-column supercritical fluid chromatography; Stationary phases; Click chemistry; Linear solvation energy relationships; Pharmaceuticals.

1. Introduction

In recent years, *click* chemistry has become an evermore popular reaction to join small units together in synthesis. A reaction to be termed as '*click* chemistry' must meet the following criteria: the reaction must be modular, wide in scope, give very high yields, generate only inoffensive byproducts that can easily be removed, and be stereospecific. Moreover, the reaction process must include simple reaction conditions, use readily available starting materials and reagents, use of no solvent or a solvent that is benign or easily removed, and have simple product isolation[1,2]. There are several classes of reactions that meet these criteria: cycloadditions of unsaturated species, nucleophilic substitution chemistry, 'non-aldol' carbonyl chemistry, and additions to carbon – carbon multiple bonds[2-4]. For the purpose of this project, focus was emphasized on the copper (I) catalyzed cycloaddition of azides to alkynes, which provides a powerful *click* chemistry tool with remarkably broad scope and exquisite selectivity for the conjugation between an appropriately functionalized terminal alkyne and organic azide, to form a 1,4-disubstituted 1,2,3-triazole ring[5-8]. This reaction has even been termed the best *click* reaction to date[9]. One of the most commonly used methods to generate the active catalyst is to use a copper (II) salt, which is reduced *in situ* with sodium ascorbate to form a copper (I) salt[2-4] (Scheme 1).

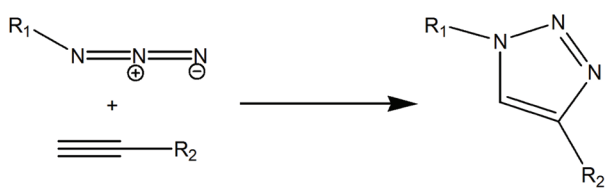

Scheme 1. Formation of the 1,4-disubstituted 1,2,3-triazole ring.

This *click* reaction has also made its way into the chromatographic arena. Several publications have reported the use of *click* chemistry for the synthesis of stationary phases for HPLC including reversed-phase, hydrophilic interaction and weak cation-exchange supports[5,6,10-13]. We recently described the synthesis by *click* chemistry of estradiol and testosterone phases for affinity LC of tripodal receptors[14].

Packed-column supercritical fluid chromatography (pSFC), pioneered by Klesper et al.[15], has been around for over 25 years and is intensively used for some specific applications, for example, chiral separations in the pharmaceutical industry. In recent years, its popularity has increased mainly because of its green character. SFC is environmentally friendly and minimizes the use of toxic organic solvents and additives, with their concomitant risks of laboratory worker exposure and disposal problems. The main instrument manufacturers recently introduced new high-performance SFC instrumentation and the technique is presently experiencing a boom as complementary method to reversed-phase LC and HILIC.

Although nearly all HPLC columns have been used in analytical pSFC, silica-based normal-phase stationary phases i.e. bare silica, diol- and cyanopropyl-bonded silica have been mostly applied until ten years ago. In attempts to avoid or reduce the use of acidic and basic additives, dedicated pSFC phases were synthesized and became commercially available. In 2001, Princeton Chromatography (Cranbury, NJ, USA) introduced a 2-ethyl pyridine stationary phase and many basic pharmaceuticals could be eluted with excellent peak shape without addition of an additive. A number of other phases (amide, urea, etc.) were synthesized to provide alternative selectivities while other small companies entered the field by synthesizing SFC dedicated stationary phases e.g. Zymor (Wayne, NJ, USA) and ES Industries (Berlin, NJ, USA). More recently, Waters (Milford, MA, USA) announced a line of Viridis SFC columns (including 2-ethyl pyride silica) and Phenomenex (Torrance, CA, USA) introduced a series of phases specially designed for SFC. A recent review of column developments for SFC can be found in ref [16].

As it has only been in the last few years that *click* chemistry has been used as a means to develop stationary

phases, it is not surprising that stationary phases for pSFC have not yet been developed by this method. The objective of this work was to use the fast, simple and versatile copper (I) catalyzed azide-alkyne cycloaddition reaction to synthesize some new, unique and tailored stationary phases for pSFC. The functionalities selected are pyridine, phenol, aniline and morpholine. Pyridine and morpholine stationary phases are commercially available but the way of linking to silica is completely different. On the other hand, other reasons to synthesize the phases are (i) batch-to-batch variability of commercially available phases making implementation in a drug discovery laboratory problematic, (ii) substantial bleeding of commercial phases in SFC-MS hypenation and (iii) the need for larger quantities of the stationary phases for semi-prep SFC. The phases were evaluated through a study of their interaction capabilities with the help of linear solvation energy relationships (LSERs)[17-19]. The *click* phases have also been compared to commercially available silica and 1,2,4-triazole-silica, both developed for HILIC, and to 2-ethyl pyridine silica.

2. Experimental

2.1. Materials

Propargyl bromide solution (~80% in toluene), morpholine (> 99.0%), 2-ethynyl pyridine (> 99.0%), dimethylformamide (DMF), dichloromethane (DCM), diphenyleneiodonium chloride (DPI), hydrochloric acid, methanol, pyridine, acetic acid anhydride, sodium azide, 6-bromohexanoic acid, and sodium ascorbate were obtained from Sigma-Aldrich, Munich, Germany). 3-ethynylphenol (>95%) and 3-ethynylaniline (98%) were purchased from Acros, Geel, Belgium. Fuji Chromatorex aminopropyl silica (5 µm d_p) was from Fuji Silysia Chemical (Kasugai, Japan), and benzotriazole-1-yl-oxy-tris-pyrrolidino-phosphonium hexafluorophosphate (PyBOP) was obtained from Merck Biosciences (Darmstadt, Germany).

One hundred and twenty seven compounds (Table 1) used for LSER characterization were obtained from a variety of manufacturers. Individual solutions of these compounds were prepared in methanol and stored at 4°C. For details on solute selection, please refer to[19]. The acidic (ibuprofen, fenoprofen, flurbiprofen and ketoprofen), basic (caffeine, theophylline and theobromine) and neutral (cortisone, prednisone, hydrocortisone and prednisolone) model solutes were from Sigma-Aldrich, (Munich, Germany) Stock solutions at concentrations between 1 and 5 mg/L were prepared in methanol and stored at 4°C and then further diluted in methanol. Metoclopromide and its impurities were obtained from LGC Standards (Molsheim, France).

A 2-ethyl pyridine column (25 cm x 4.6 mm i.d., 5 µm d_p) was purchased from Bischoff (Leonberg, Germany), a Cosmosil HILIC triazole column (15 cm x 4.6 mm i.d., 5 µm d_p) was purchased from Nacalai USA, Inc. (San Diego, CA, USA) and a bare silica RXSIL column (15 cm x 4.6 mm i.d., 3 µm d_p) was obtained from Agilent Technologies (Brussel, Belgium). High purity liquid carbon dioxide was obtained from Air Liquide (Herenthout, Belgium).

2.2. Instrumentation

A Mettler-Toledo TGA (Model SDTA851e, Mettler-Toledo, Zaventem, Belgium) controlled by STAR software provided with the instrument (version SW 9.00) was utilized for the thermogravimetric analysis of the synthesized stationary phases. The conditions were as follows: approximately 3 mg of sample was weighed out and the temperature range was from 25 – 1100°C at 10°C/min.

The SFC system used for LSER characterization was described elsewhere[18]. The conditions were as follows: injection was 1 µL, the CO_2-methanol 90:10 (v/v) mobile phase flow rate was isocratic at 3 mL/min, the outlet pressure was 150 bar, detection wavelength was 254 nm, and the temperature was isothermal at 25°C. These conditions were chosen to match the conditions used to establish a column classification for SFC[18] so as to provide comparison points.

Table 1. Supplement: List of compounds used for LSER characterization.

No	Compound	E	S	A	B	V
1	Benzene	0.610	0.52	0.00	0.14	0.7164
2	Toluene	0.601	0.52	0.00	0.14	0.8573
3	Ethylbenzene	0.613	0.51	0.00	0.15	0.9982
4	Propylbenzene	0.604	0.50	0.00	0.15	1.1391
5	Butylbenzene	0.600	0.51	0.00	0.15	1.2800
6	Pentylbenzene	0.594	0.51	0.00	0.15	1.4209
7	Hexylbenzene	0.591	0.50	0.00	0.15	1.5620
8	Heptylbenzene	0.577	0.48	0.00	0.15	1.7029
9	Octylbenzene	0.579	0.48	0.00	0.15	1.8438
10	Nonylbenzene	0.578	0.48	0.00	0.15	1.9847
11	Decylbenzène	0.579	0.47	0.00	0.15	2.1256
12	Undecylbenzene	0.579	0.47	0.00	0.15	2.2665
13	Dodecylbenzene	0.571	0.47	0.00	0.15	2.4074
14	Tridecylbenzene	0.570	0.47	0.00	0.15	2.5483
15	Tetradecylbenzene	0.570	0.47	0.00	0.15	2.6892
16	Allylbenzene	0.717	0.60	0.00	0.22	1.0961
17	Cumene	0.602	0.49	0.00	0.16	1.1391
18	*t*-Butylbenzene	0.614	0.49	0.00	0.16	1.28
19	*o*-Xylene	0.663	0.56	0.00	0.16	0.9980
20	*m*-Xylene	0.623	0.52	0.00	0.16	0.9980
21	*p*-Xylene	0.613	0.52	0.00	0.16	0.9980
22	Naphthalene	1.340	0.92	0.00	0.20	1.0854
23	1-Methylnaphthalene	1.344	0.90	0.00	0.20	1.2260
24	2-Methylnaphthalene	1.304	0.92	0.00	0.20	1.2260
25	1-Ethylnaphthalene	1.371	0.87	0.00	0.20	1.3670
26	2-Ethylnaphthalene	1.331	0.87	0.00	0.20	1.3670
27	Aniline	0.955	0.96	0.26	0.50	0.8162
28	N,N-Dimethylaniline	0.957	0.84	0.00	0.47	1.0980
29	Pyridine	0.631	0.84	0.00	0.52	0.6753
30	2-Ethylpyridine	0.613	0.70	0.00	0.49	0.9570
31	Phenylurea	1.110	1.40	0.77	0.77	1.0730
32	Caffeine	1.500	1.60	0.00	1.35	1.3630
33	Nicotinamide	1.010	1.09	0.63	1.00	0.9317
34	Indazole	1.180	1.25	0.54	0.34	0.9050
35	Carbazole	1.787	1.42	0.47	0.26	1.3150
36	Acridine	2.356	1.32	0.00	0.58	1.4130
37	*o*-Toluidine	0.966	0.92	0.23	0.45	0.957
38	*m*-Toluidine	0.946	0.95	0.23	0.55	0.957
39	*p*-Toluidine	0.923	0.95	0.23	0.52	0.957
40	Naphtylamine	1.670	1.26	0.20	0.57	1.1850
41	Benzoic acid	0.730	0.90	0.59	0.40	0.9317
42	Naphtoic acid	1.200	1.27	0.52	0.48	1.3007
43	Naphtylacetic acid	1.300	1.35	0.54	0.40	1.3007

Table 1. Supplement: List of compounds used for LSER characterization.

No	Compound	E	S	A	B	V
44	Anisole	0.708	0.75	0.00	0.29	0.9160
45	Phenylethanol	0.784	0.83	0.30	0.66	1.0570
46	Benzyl alcohol	0.803	0.87	0.39	0.56	0.9160
47	Benzaldehyde	0.820	1.00	0.00	0.39	0.8730
48	Acetophenone	0.818	1.01	0.00	0.48	1.0139
49	Propiophenone	0.804	0.85	0.00	0.51	1.1548
50	Valerophenone	0.795	0.95	0.00	0.50	1.4366
51	Coumarine	1.060	1.79	0.00	0.46	1.0620
52	Benzonitrile	0.742	1.11	0.00	0.33	0.8711
53	Nitrobenzene	0.871	1.11	0.00	0.28	0.8906
54	Chlorobenzene	0.718	0.65	0.00	0.07	0.8288
55	Bromobenzene	0.882	0.73	0.00	0.09	0.8910
56	Iodobenzene	1.188	0.82	0.00	0.12	0.9750
57	*o*-Methylacetophenone	0.780	1.00	0.00	0.51	1.1550
58	*m*-Methylacetophenone	0.806	1.00	0.00	0.51	1.1550
59	*p*-Methylacetophenone	0.842	1.00	0.00	0.52	1.1550
60	Benzophenone	1.447	1.50	0.00	0.50	1.4810
61	Naphthalene methanol	1.640	1.19	0.27	0.64	1.2850
62	Naphthalene ethanol	1.670	1.21	0.23	0.72	1.4259
63	Naphtylaldehyde	1.470	1.19	0.00	0.47	1.2420
64	Naphtylacetate	1.130	1.25	0.00	0.62	1.4416
65	Cyanonaphthalene	1.190	1.25	0.00	0.41	1.2401
66	Naphtylacetonitrile	1.430	1.44	0.00	0.53	1.3810
67	Nitronaphthalene	1.600	1.51	0.00	0.29	1.2596
68	Fluoronaphthalene	1.320	0.82	0.00	0.18	1.1030
69	Chloronaphthalene	1.540	0.92	0.00	0.15	1.2078
70	Bromonaphthalene	1.670	0.97	0.00	0.17	1.2604
71	Iodonaphthalene	1.840	1.04	0.00	0.20	1.3436
72	Phenol	0.805	0.89	0.60	0.30	0.7751
73	Eugenol	0.946	0.99	0.22	0.51	1.3540
74	Vanillin	1.040	1.04	0.32	0.67	1.1313
75	Resorcinol	0.980	1.00	1.10	0.58	0.8340
76	α-Naphtol	1.520	1.05	0.61	0.37	1.1441
77	β-Naphtol	1.520	1.08	0.61	0.40	1.1440
78	*o*-Cresol	0.840	0.86	0.52	0.30	0.9160
79	*m*-Cresol	0.822	0.88	0.57	0.34	0.9160
80	*p*-Cresol	0.820	0.87	0.57	0.31	0.9160
81	2,3-Dimethylphenol	0.850	0.85	0.52	0.36	1.0569
82	2,4-Dimethylphenol	0.840	0.80	0.53	0.39	1.0570
83	2,5-Dimethylphenol	0.840	0.79	0.54	0.37	1.0570
84	2,6-Dimethylphenol	0.860	0.79	0.39	0.39	1.0570
85	3,4-Dimethylphenol	0.830	0.86	0.56	0.39	1.0570
86	3,5-Dimethylphenol	0.820	0.84	0.57	0.36	1.0570

Table 1. Supplement: List of compounds used for LSER characterization.

No	Compound	E	S	A	B	V
87	*o*-Isopropylphenol	0.822	0.79	0.52	0.44	1.1978
88	*m*-Isopropylphenol	0.811	0.92	0.55	0.46	1.1978
89	*p*-Isopropylphenol	0.791	0.89	0.55	0.38	1.1978
90	*o*-Chlorophenol	0.853	0.88	0.32	0.31	0.8975
91	*m*-Chlorophenol	0.909	1.06	0.69	0.15	0.8975
92	*p*-Chlorophenol	0.915	1.08	0.67	0.20	0.8975
93	*o*-Nitrophenol	1.045	1.05	0.05	0.37	0.9490
94	*m*-Nitrophenol	1.050	1.57	0.79	0.23	0.9490
95	*p*-Nitrophenol	1.070	1.72	0.82	0.26	0.9490
96	*o*-Nitrobenzylalcohol	1.059	1.11	0.45	0.65	1.0900
97	*m*-Nitrobenzylalcohol	1.064	1.35	0.44	0.64	1.0900
98	*p*-Nitrobenzylalcohol	1.064	1.39	0.44	0.62	1.0900
99	*o*-Nitrotoluene	0.866	1.11	0.00	0.28	1.0320
100	*m*-Nitrotoluene	0.874	1.10	0.00	0.25	1.0320
101	*p*-Nitrotoluene	0.870	1.11	0.00	0.28	1.0320
102	Methylbenzoate	0.733	0.85	0.00	0.48	1.0726
103	Ethylbenzoate	0.689	0.85	0.00	0.46	1.2140
104	Propylbenzoate	0.675	0.80	0.00	0.46	1.3540
105	Butylbenzoate	0.668	0.80	0.00	0.46	1.4953
106	Benzylbenzoate	1.264	1.42	0.00	0.51	1.6804
107	Dimethylphthalate	0.780	1.41	0.00	0.88	1.4290
108	Diethylphthalate	0.729	1.40	0.00	0.88	1.7110
109	Dipropylphthalate	0.713	1.40	0.00	0.86	1.9924
110	Dibutylphthalate	0.700	1.40	0.00	0.86	2.2700
111	Biphenyl	1.360	0.99	0.00	0.26	1.3242
112	Phenyl-naphthalene	1.910	1.08	0.00	0.30	1.6932
113	Acenaphthene	1.604	1.05	0.00	0.22	1.1726
114	Acenaphtylene	1.750	1.14	0.00	0.26	1.2156
115	Fluorene	1.588	1.03	0.00	0.20	1.3570
116	Phenanthrene	2.055	1.29	0.00	0.26	1.4540
117	Anthracene	2.290	1.34	0.00	0.26	1.4540
118	9-Methylanthracene	2.290	1.30	0.00	0.26	1.5950
119	Fluoranthene	2.377	1.53	0.00	0.20	1.5850
120	Pyrene	2.808	1.71	0.00	0.29	1.5850
121	Chrysene	3.027	1.73	0.00	0.36	1.8230
122	Benzo[a]pyrene	3.625	1.98	0.00	0.44	1.9536
123	Perylene	3.256	1.76	0.00	0.42	1.9536
124	Binaphthyl	2.820	1.81	0.00	0.31	2.0622
125	Triphenylene	3.000	1.71	0.00	0.42	1.8234
126	o-Terphenyl	2.194	1.61	0.00	0.38	1.9320
127	p-Terphenyl	2.194	1.61	0.00	0.38	1.9320

E: Excess molar refraction; S: Dipolarity/polarizability; A: Hydrogen bond acidity; B: Hydrogen bond basicity (McGowan's characteristic); V: Volume.

Other analyses were performed on a SFC system composed of a Sandra/Selerity 5000 SFC pump (Selerity Technologies, Salt Lake City, UT, USA), an Agilent 1200 HPLC system equipped with a high pressure cell and variable wavelength detector (Agilent Technologies, Brussels, Belgium), a Gerstel Multipurpose Sampler (MPS-3) autosampler (Mülheim an der Ruhr, Germany), and a Polaratherm column oven with mobile phase pre-heater (Selerity Technologies). SFC separation conditions are outlined in references[20,21] and in the text. An Agilent 1969A Orthogonal TOF mass spectrometer with APCI source (Agilent Technologies) was utilized for the analysis of the metoclopromide sample. The conditions for the source were as follows: capillary voltage 3000 V, source temperature 350°C, vaporization temperature 350°C, corona current 7 mA, flow rate of the nebulizer gas (N_2) 7 L/min and nebulizer pressure 50 psi.

2.3. Data analysis

The LSER coefficients were obtained by multiple linear regression analysis on the logarithm of the measured retention factors (log *k*), carried out with XLSTAT 7.5 software (Addinsoft, New York, NY, USA). As recommended by recent reviews[22], the quality of the fits was estimated using the multiple correlation coefficient (R^2), adjusted determination coefficient (R^2_{adj}), standard error in the estimate (*SE*) and Fischer *F* statistic.

2.4. Synthesis of the stationary phases

The synthesis is based on the procedures described previously for estradiol and testosterone *click* stationary phases[14].

2.4.1. Morpholine precursor

The procedure by Verron et al.[23] was followed, though scaled-down, for the synthesis of morpholine precursor 4-prop-2-ynyl-morpholine (Scheme 2).

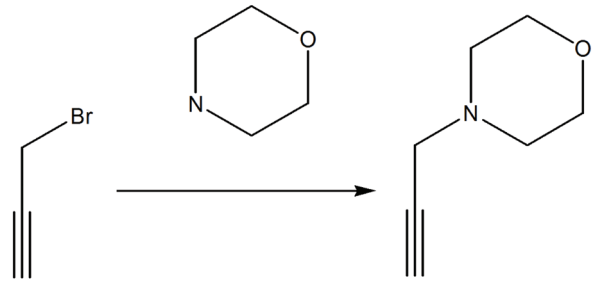

Scheme 2. Synthesis of 4-prop-2-ynyl-morpholine.

Morpholine (25 mL, 29 mmol) was dissolved in MeOH (250 mL) while cooled in ice and under an inert atmosphere. Once dissolved, potassium carbonate (21.9 g, 16 mmol) and propargyl bromide (31 mL, 29 mmol) were added with stirring while cooling was maintained. Stirring without cooling was continued for 4 h. The precipitate was filtered and washed with MeOH. The MeOH was removed by rotavap at 40°C. The precipitate was filtered using DCM (sonication was required to remove the precipitate from the round bottom flask). The DCM was then removed via rotavap at 40°C. The yellow oil remaining after completion was stored at 4°C. A percent yield of 83% was obtained.

GC-MS and NMR analysis were performed on the oil. The GC-MS chromatogram contained a single peak with only the final product present. No starting material was observed. The ^{1}H NMR shifts matched those reported by Verron et al.[23]. ^{1}H NMR (300 MHz, $CDCl_3$): δ = 2.27 (d, 1H, CCH), δ = 2.57 (t, 4H, CH_2N), δ = 3.29 (d, 2H, $CCCH_2$), δ = 3.75 (t, 4H, CH_2O). ^{13}C NMR (300 MHz, $CDCl_3$): δ = 47.19 (s, 1C, CCH_2N), δ = 52.19 (s, 2C, CH_2N), δ = 66.84 (s, 2C, CH_2O), δ = 73.35 (s, 1C, $CCCH_2$), δ = 78.46 (s, 1C, $CCCH_2$).

2.4.2. Synthesis of 6-azidohexanoic acid.

6-azidohexanoic acid was synthesized according to Scheme 3.

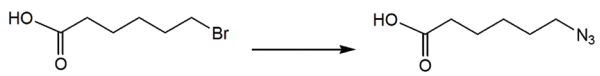

Scheme 3. Synthesis of 6-azidohexanoic acid.

Sodium azide (4.00 g, 62 mmol) and 6-bromohexanoic acid (6.00 g, 31 mmol) were combined in a reaction vessel with 40 mL DMF. A condenser was placed atop the reaction vessel and the reaction was stirred in an oil bath at 85°C overnight.

A liquid-liquid extraction was carried out in a separation funnel. DCM was used to extract out the product 6-azidohexanoic acid. The DCM extraction was carried out three times, and the DCM layers from each extraction were combined. Then 0.1 M HCl was used to extract the DMF from the collected DCM layers. This extraction was also carried out three times, and the DCM layers were collected. Magnesium sulfate was added to the DCM layer with stirring to dry the solvent. This was then filtered, and the DCM layer containing the final product was rotavaped at 40°C. A yellow oil was obtained. This synthesis was also performed in a scaled-up reaction. The average percent yield obtained was 72%.

^{1}H NMR and IR analyses were performed on the oil. ^{1}H NMR (300 MHz, $CDCl_3$): δ = 1.45 (m, 2H, $CH_2(CH_2)_2$), δ = 1.67 (m, 4H, $CH_2(CH_2)_2$), δ = 2.38 (t, 2H, CH_2CO), δ = 3.29 (m, 2H, CH_2N_3). The IR spectra contained a band at 2093 cm^{-1}, which corresponds to the presence of an azide.

2.4.3. Attachment of 6-azidohexanoic acid to the aminopropyl silica particles (Scheme 4)

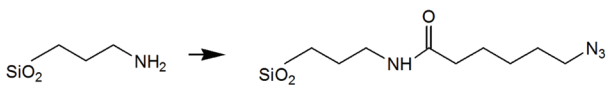

Scheme 4. Attachment of 6-azidohexanoic acid to aminopropyl silica particles.

Based on the amine loading (C 4.4%, N 1.3%) of the silica particles used, the ratio was 1:3:3:6 amino groups: 6-azidohexanoic acid: PyBOP: DPI. Thus, aminopropyl silica (10 g, 12 mmol amine), 6-azidohexanoic acid (5.65 g, 36 mmol), PyBOP (18.70 g, 36 mmol), and DPI (12.5 mL, 72 mmol) were all combined in 144 mL DMF. This reaction was shaken at room temperature for 4.5 h. The particles were filtered using a size 4 filter. The particles were washed three times each with DMF, MeOH, and DCM. The particles were then allowed to dry in an oven at 60°C before endcapping occurred. To endcap, the entire product from the above reaction was combined with 10 mL pyridine, 30 mL acetic acid anhydride, and 60 mL DMF. This reaction was shaken at room temperature for 1 h. The particles were filtered using a size 4 filter. The particles were washed three times each with DMF, MeOH, and DCM, and then dried in an oven at 60°C.

A color test was performed to determine if free amines were still present[24,25]. To the endcapped aminopropyl silica modified with 6-azidohexanoic acid, 3 drops of picrylsulfonic acid (TNBS) solution and 5 drops of 10% DIEA/DMF solution were added. The picrylsulfonic acid will only react with free amines, giving a color (red) change. No color change was observed.

2.4.4. Clicking stationary phases to the azide-modified particles (Scheme 5)

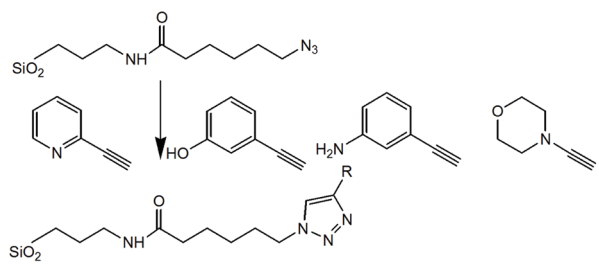

Scheme 5. *Clicking* pyridine, phenol, aniline and morpholine.

All of the particles from the endcapping step were utilized for the *click* reaction: 4-prop-2-ynyl morpholine (7.5 g, 60 mmol), copper sulfate pentahydrate (3.0 g, 12 mmol), and sodium ascorbate (12.0 g, 60 mmol) were combined with the particles in 240 mL 1:1 water:isopropanol. This material is referred to as *clicked* morpholine (C-Mor). For the other stationary phases, 2-ethynyl pyridine (6.1 g, 60 mmol) was used for the *clicked* pyridine (C-Pyr) phase, 3-ethynyl phenol (6.9 g,

60 mmol) for the *clicked* phenol (C-Phe) phase, and 3-ethynyl aniline (7.1 g, 60 mmol) for the *clicked* aniline phase (C-Anal). All other conditions were the same as for the C-Mor phase. After 24 h, the particles were filtered with a size 4 filter and washed three times each with DMF, MeOH, and DCM. However, the particles still contained Cu^{2+} from the catalyst used in the *click* reaction. Therefore, the particles were suspended in a 0.1 M EDTA solution. This was allowed to shake overnight at room temperature. The particles were then filtered and washed three times each with water, MeOH, and DCM. The particles were then allowed to dry at 60°C for 1 h. The synthesized stationary phases (i.e.C-Pyr, C-Phe, C-Anil and C-Mor) were packed into 15 cm x 3 mm i.d. columns by Mel Euerby from HiChrom (Berkshire, UK).

3. Results and discussion

3.1. Thermogravimetric analysis (TGA)

Thermogravimetric analysis (TGA) was performed to determine the load of the *click* reactions on the aminopropyl silica. All phases show an increase with ca. 10% compared to the aminopropyl silica as such (Figure 1).

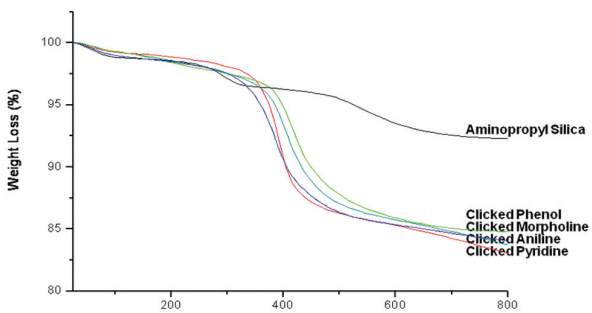

Figure 1. Thermogravimetric analysis (TGA) plots of the synthesized *click* stationary phases.

3.2. LSER characterization

The QSRR (quantitative structure-retention relationship) approach furnishes a detailed and reliable description of the role and extent of the different molecular interactions that can be established between the analytes and the chromatographic system. Among QSRRs, the solvation parameter model using Abraham descriptors has gained acceptance as a general tool to explore the factors affecting retention in chromatographic systems[20]. The retention of selected probes in a dense fluid can be related through this relationship, also known as linear solvation energy relationship (LSER), to specific interactions by the following equation:

$$\log k = c + eE + sS + aA + bB + vV \quad (1)$$

In this equation, capital letters represent the solute descriptors, related to particular interaction properties, while lower case letters represent the system constants, related to the complementary effect of the phases on these interactions. *c* is the model intercept term, which when the retention factor is used as the dependent variable is dominated by the phase ratio. E is the excess molar refraction (calculated from the refractive index of the molecule) and models polarizability contributions from *n* and ϖ electrons; S is the solute dipolarity / polarizability; A and B are the solute overall hydrogen-bond acidity and basicity; V is the McGowan characteristic volume in units of $cm^3\ mol^{-1}/100$. The system constants (*e*, *s*, *a*, *b*, *v*), obtained through a multilinear regression of the retention data for a certain number of solutes with known descriptors, reflect the magnitude of difference for that particular property between the mobile and stationary phases. Thus, if a particular coefficient is numerically large, then any solute having the complementary property will interact very strongly with either the mobile phase (if the coefficient is negative) or the stationary phase (if the coefficient is positive). Eq. (2) can be deduced from Eq. (1):

$$\log\alpha = e\Delta E + s\Delta S + a\Delta A + b\Delta B + v\Delta V \quad (2)$$

where α is the separation factor between two solutes and ΔX represents the difference in the X coefficient between these two solutes. Consequently, the coefficients also reflect the system's selectivity towards any particular molecular interaction.

Moreover, characterising different stationary phases while always using the same mobile phase and

operating conditions ensures that the LSER coefficients can be compared to provide a comparison of the stationary phase properties. Numerous stationary phases have been evaluated with this method in SFC conditions[18,19], to provide a classification of stationary phases for pSFC uses.

Furthermore, based on[26], the angle between two solvation vectors (ω) associated to two chromatographic systems can be calculated according to the following equation, based on the solvation parameter model coefficients of the two systems noted i and j:

$$\cos\theta_{ij} = \frac{\vec{\omega}_i * \vec{\omega}_j}{|\vec{\omega}_i| * |\vec{\omega}_j|} = \frac{e_i e_j + s_i s_j + a_i a_j + b_i b_j + v_i v_j}{\sqrt{e_i^2 + s_i^2 + a_i^2 + b_i^2 + v_i^2}\sqrt{e_j^2 + s_j^2 + a_j^2 + b_j^2 + v_j^2}} \quad (3)$$

The angle between two columns provides a mean to measure the informational equivalence of different chromatographic systems. However, this information is not sufficient to judge whether two stationary phases are similar, as it does not take into account the confidence limits associated to the system constants.

The similarity between two chromatographic systems is thus evaluated through the calculation of the J similarity factor, determined through Eqs. (4), (5) and (6):

$$J = \cos\theta_{ij} - \cos(\theta_{di} + \theta_{dj}) \quad (4)$$

$$\cos(\theta_{di} + \theta_{dj}) = \sqrt{\left(1 - \frac{D_i^2}{|\vec{\omega}_i|^2}\right)\left(1 - \frac{D_j^2}{|\vec{\omega}_j|^2}\right)} - \frac{D_i D_j}{|\vec{\omega}_i||\vec{\omega}_j|} \quad (5)$$

$$D = TINV(1 - 0.99, N) \bullet SE \quad (6)$$

where TINV is the inverse of the Student's t-distribution for the specified degrees of freedom N, and SE is the average of the standard errors of the solvation parameter model coefficients.

In Eq. (4), when J is positive, the systems compared are found to be similar; in the opposite case, they are considered to be different.

When two stationary phases are similar, it indicates that the elution order of analytes will be very similar on the two chromatographic systems. However, retention might be different. The global intensity of the interactions can be compared through the values of the solvation vector length, calculated as follows:

$$u_i = \sqrt{e_i^2 + s_i^2 + a_i^2 + b_i^2 + v_i^2} \quad (7)$$

Thus when u_i and u_j are close, retention will be similar on both phases (provided phase ratio is close), while different values of vector length indicates that retention and separation factors will be larger on the chromatographic system providing larger values of *u*.

The results obtained with the commercially available 2-ethyl pyridine column, 1,2,4-triazole column and bare silica column were compared to those obtained with the *clicked* columns. The 2-ethyl pyridine column was chosen for the purpose of comparison because one of the *click* stationary phases has a pyridine ring as a terminal function, and because it is a very popular column among SFC users. The 1,2,4-triazole column was also an interesting comparison point because it has a triazole ring as the stationary phase, whereas with the *clicked* columns, a triazole ring is embedded in the linker. Note, however, that the comparison cannot be completely correct as the 1,2,3-triazole ring in the *click* phases has a pKa of 1.2 while the 1,2,4-triazole ring has a pKa of 2.2.

All the models calculated for the six stationary phases (the four *click* stationary phases, and the 2-ethyl pyridine and 1,2,4-triazole phase) in this study are presented in Table 2, together with the statistics of the regression equations.

The fits for the click stationary phases were all of reasonable quality, R^2_{adj} ranging from 0.933 to 0.964, standard error in the estimate varying from 0.109 to 0.147. All coefficients are significantly larger than their standard deviation; therefore, the results are amenable to interpretation. Only few outliers were eliminated from the models but, in any case, always more than

Table 2. System constants and model fit statistics.

Stationary phase	*c*	*e*	*s*	*a*	*b*	*v*	n	R^2	R^2_{adj}	*SE*	*F*	*u*
C-Phenol	-1.245	0.604	0.208	1.222	0.749	-0.247	115	0.936	0.933	0.145	319	1.59
	0.069	*0.038*	*0.071*	*0.060*	*0.081*	*0.054*						
C-Aniline	-1.340	0.540	0.426	1.506	0.409	-0.143	108	0.966	0.964	0.109	573	1.71
	0.056	*0.031*	*0.063*	*0.048*	*0.068*	*0.041*						
C-Morpholine	-1.155	0.537	0.214	1.654	0.359	-0.254	117	0.939	0.937	0.147	343	1.81
	0.067	*0.038*	*0.072*	*0.060*	*0.081*	*0.052*						
C-Pyridine	-1.345	0.528	0.247	1.648	0.298		113	0.949	0.947	0.131	506	1.77
	0.041	*0.033*	*0.064*	*0.049*	*0.072*							
2-ethyl pyridine	-1.057	0.588	0.564	1.053	0.790	-0.692	120	0.929	0.926	0.191	297	1.70
	0.086	*0.050*	*0.094*	*0.069*	*0.120*	*0.071*						
1,2,4-triazole	-1.244	0.595		1.556	1.037	-0.491	100	0.934	0.932	0.136	339	2.02
	0.067	*0.031*		*0.058*	*0.086*	*0.068*						

n is the number of solutes considered in the regression, R^2 is the multiple correlation coefficient, R^2_{adj} is the adjusted correlation coefficient, *SE* in the standard estimate error, *F* is Fischer's statistic and the numbers in italics represent 99% confidence limits, is the length of the vector associated to the chromatographic system, calculated according to equation (7).

100 compounds were retained in the final model calculation, and the diversity of chemical functions is unaltered by the removal of outliers, thus all conclusions should be highly substantial.

Using the solvation parameter model, the different chromatographic systems can be compared based on the values of the regression coefficients. First of all, it can be noticed that all polar-type interactions (*e*, *s*, *a*, *b*) are positive, indicating that they are stronger between analytes and stationary phase than between analytes and mobile phase, while the dispersive interactions (*v*) are negative or zero. This pattern is classical with polar stationary phases characterized in supercritical mobile phases: an increase in polarity of the analytes causes an increase in retention, while an increase in hydrocarbon volume causes a decrease in retention.

The *a* coefficient is the largest on all columns, indicating significant basic character of the stationary phases. Second most important coefficients are *b* (indicating acidic character of the stationary phase) or *e*, due to the aromatic character of all stationary phases.

The θ_{ij} angles existing between the solvation vectors associated to all the stationary phases characterized above through the use of the solvation parameter model and the *J* similarity factors at the 99% confidence limit between them were calculated, according to Eqs. (3) to (6). They can be observed in Table 3.

Based on angle calculation, C-Pyr cannot be discriminated from C-Mor. They display a 8° angle between them with slightly larger *u* vector length for C-Mor. This is also visible on the κ-κ plot (Figure 2A). The slope is close to 1, indicating generally similar interaction strength on the two phases. The intercept is positive indicating larger retention on C-Pyr than on C-Mor. The position of the regression line above the first bisector can possibly be related to a larger *v* coefficient. This is possibly due to the C-Pyr phase being somewhat less cohesive than the others, as will be discussed further below. In this case, solutes penetrate more easily in the stationary phase and are more retained.

The 2-ethyl pyridine stationary phase is significantly different from the *click* stationary phases, and in particular, it is very different from the C-Pyr stationary phase, with a measured angle of 36° between them. The κ-κ plot comparing the two pyridine-type phases (Figure 2B) indeed shows important differences between the two columns.

Table 3. Values of the θ angles between the solvation vectors.

θ_{ij}	C-Phenol	C-Aniline	C-Morpholine	C-Pyridine	2-ethyl pyridine	1,2,4-triazole
C-Phenol		17	18	22	21	11
C-Aniline	17		10	16	22	22
C-Morpholine	18	10		**8***	31	22
C-Pyridine	22	16	**8***		36	27
2-ethyl pyridine	21	22	31	36		23
1,2,4-triazole	11	22	22	27	23	

θ is calculated according to equation (3). The asterisks indicate the couples judged similar through the calculation of J, according to equations (4), (5) and (6), at the 99% confidence limit.

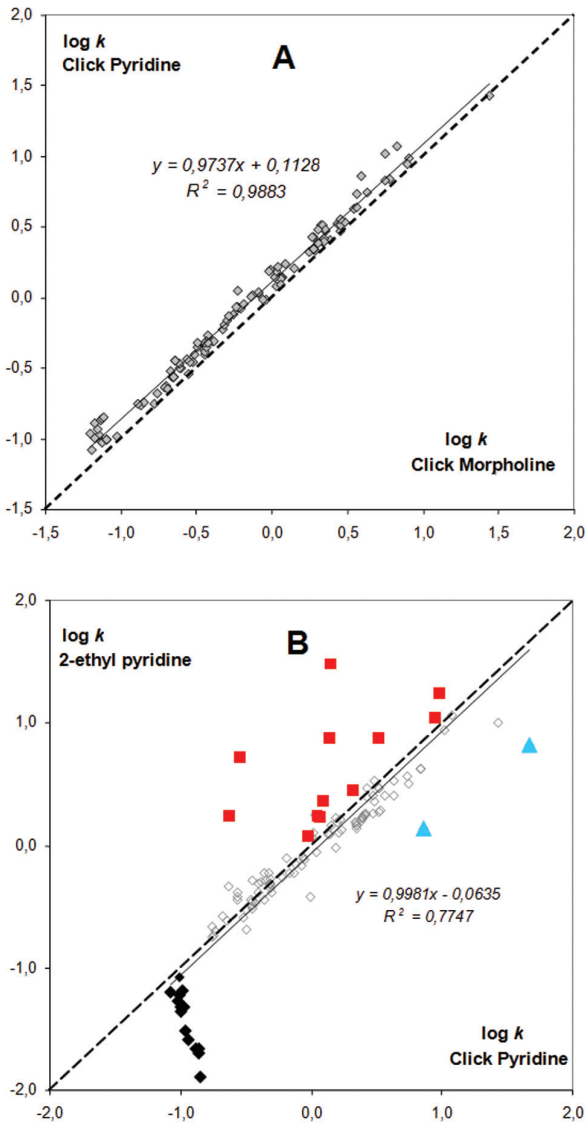

Figure 2. Comparison of the retention factors (log *k* – log *k* plots) for all compounds in Table 1 between (A) *click* Pyridine and *click* Morpholine and (B) 2-ethyl pyridine and *click* Pyridine. Black diamonds are alkylbenzenes (compounds 1 to 15 in Table 2); blue triangles are acidic solutes (n° 41 and 42 in Table 2); red squares are basic analytes (compounds 27 to 40 in Table 2).

Phase ratio seems quite close between the two columns, as most points are close to the first bisector, but three compound families exhibit different behaviours: (i) the alkylbenzene homologous series indicate that methylene selectivity is nearly zero on *click* Pyridine (which is consistent with a zero value of the *v* coefficient) while it is negative on 2-ethyl pyridine (in accordance with the significant negative *v* value); (ii) basic solutes are more retained on the 2-ethyl pyridine phase, as indicated by the largest *b* coefficient on 2-ethylpyridine and (iii) acidic solutes are more retained on the C-Pyr phase, as indicated by the largest *a* coefficient.

Judging from the angle values, the 1,2,4-triazole phase is also significantly different from the *click* phases, indicating significant contribution of the terminal ligand to retention on the *click* phases. However, the angles are smaller between *click* phases and 1,2,4-triazole than between *click* phases and 2-ethylpyridine. C-Pyr appears to be the closest to the 1,2,4-triazole phase, with 11° and 13° angles respectively.

Further information can be retrieved from a close examination of the LSER coefficients.

The *c* constant does not vary significantly between the five click columns and will thus not be discussed.

3.2.1. The e coefficient

This coefficient does not vary significantly among the six phases (bare silica is included for comparison, see further), as can be seen on Figure 3A. This is not

surprising as the *e* coefficient only shows very little variance among all stationary phases characterized in SFC[19]. This is partly due to its composite nature (it represents dispersive, ϖ-ϖ and dipole-induced dipole interactions), and partly due to the fact that all the test solutes (Table 1) possess an aromatic group (to allow for UV detection) thus the capability to interact through ϖ and non-binding electrons cannot be correctly assessed. However, as all the stationary phases in this study also have an aromatic group or at least double-bonds and non-binding electrons, it can be expected that, even with non-aromatic solutes in the test-set, no great differences would be seen.

3.2.2. The s coefficient

This coefficient varies to a greater extent (Figure 3B). The S descriptor is associated to heterogeneous charge repartition in the analyte structure, thus the *s* coefficient represents dipole-dipole type interactions. C-Anil, in particular, is seen to provide stronger dipole-dipole and dipole-induced dipole interactions than the others. However, the strongest dipole-dipole interactions are observed on the 2-ethyl pyridine phase. On the 1,2,4-triazole phase, and only on this one, the *s* coefficient is zero, indicating that the introduction of a terminal function clearly provides some differences as compared to the triazole ring alone.

3.2.3. The a coefficient

As mentioned above, this coefficient is the largest on all phases (Figure 3C). As it indicates retention of acidic solutes, it is related to the basic character of the stationary phase, or to its ability to participate in hydrogen-bond interactions as an electron-donor. C-Phe is clearly less basic than C-Anil, C-Mor and C-Pyr, as could have been expected, based on the nature of the ligand: indeed, the phenol functional groups are naturally less basic than the nitrogen atoms of the latter three. C-Mor and C-Pyr are nearly identical. C-Anil is close to C-Mor and C-Pyr. 1,2,4-Triazole is also among the most basic phases, while the 2-ethyl pyridine phase is significantly less basic than all others. This suggests that the 1,2,3-triazole ring is taking a significant part in the basic character of the *click* stationary phases.

3.2.4. The b coefficient

This coefficient provides a variety of interactions among the tested stationary phases (Figure 3D). As it indicates retention of basic solutes, it is related to the acidic character of the stationary phase, or to its ability to participate in hydrogen-bond interactions as a proton-donor. As expected based on stationary phase structure, C-Phe is more acidic than the "basic" phases, C-Anil, C-Mor and C-Pyr.

The 1,2,4-triazole phase is the most acidic of all. The exact nature of the stationary phase structure is unknown to us, as the information provided by the manufacturer only shows the triazole ring, without any details as regards possible spacer arms. Thus we have two possible explanations: either the –NH= group from the triazole ring or residual silanol groups can be responsible for extra retention of the basic solutes on this phase.

The 2-ethyl pyridine is also among the most acidic phases, which is surprising judging that the pyridine function is not acidic. Residual silanol groups or some other functional groups could be responsible for the strong acidic character.

3.2.5. The v coefficient

This coefficient also varies to a large extent (Figure 3E), especially for the 1,2,4-triazole and 2-ethyl pyridine phases, which display large negative *v* values, and for C-Pyr, the only phase where this coefficient is zero. As it is negative on polar phases, care must be taken in the interpretation of the *v* coefficient. When it increases (decreases in absolute value), it indicates a less cohesive phase and/or more dispersive interactions.

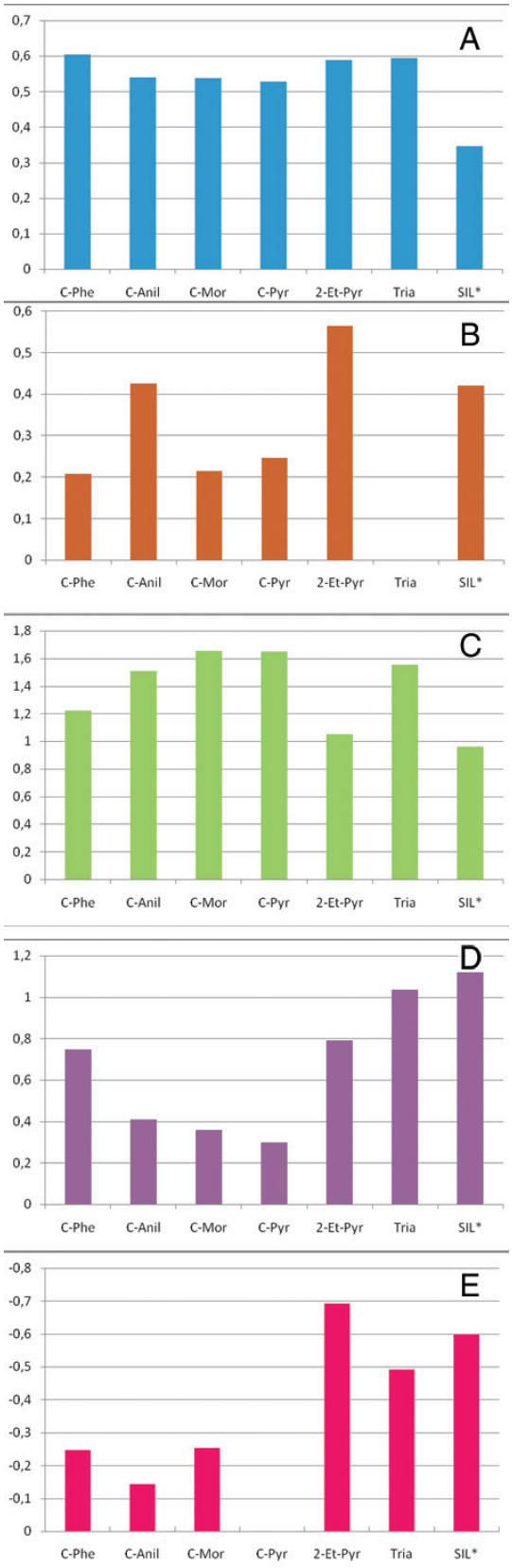

Figure 3. LSER coefficients calculated for the seven columns studied. *e* coefficient (A), *s* coefficient (B), *a* coefficient (C), *b* coefficient (D), *v* coefficient (E).

3.2.6. Systems constants for bare silica

The system constants for bare silica have been included in Figure 3 because in our opinion[20,21] and supported by recent literature on porous[27] and core shell silica particles[28], this stationary phase has unique characteristics for SFC. Moreover, its quality is presently such that acidic as well as basic solutes can be analysed by SFC without addition of additives (see further). Note in Figure 3 that silica compared to the other phases is the most proton donor (acidic) and the less proton acceptor (basic) phase.

3.3. Chromatographic analysis

The above detailed classification gives a general picture of the polarity/selectivity of the *click* phases compared to other polar, moderately polar aromatic, polar alkyl, and non-polar alkyl phases[17]. The *click* phases all belong to the polar phases in SFC or normal phases in LC. Upon injecting the 10 component standard mixture, all phases show a group separation of acids/bases from the neutral hydrophobic species. The latter elute at the end of the chromatogram and always in the same elution order i.e. cortisone, prednisone, hydrocortisone and prednisolone. A typical chromatogram is shown for the commercial 1,2,4-triazole column in Figure 4A. The same profile was obtained for the 2-ethyl pyridine, the C-Pyr and C-Mor phases. The C-Phe and C-Anil phases showed a different elution order for the acid and bases and a much more pronounced group separation for polar/neutrals. This is illustrated in Figure 4B for the analysis of the same mixture on the C-Phe column. This column showed excellent selectivity for samples of drug discovery and was experienced to have a broader applicability range compared to the C-Anil phase.

From the LSER characterization and also based on a large number of analyses of pharmaceutical samples, the C-Phe and C-Mor phases were considered most valuable for selectivity optimization for real samples.

As an example, the complementary nature of silica and C-Mor is illustrated for the analysis of an

acid/base mixture. On silica (Figure 5A), the acids elute before the bases and flurbiprofen/fenoprofen are not separated. On the C-Mor phase, the acid/base order is disturbed because the bases elute faster on this phase. For both chromatograms, no additives were used illustrating the high inertness of the phases. The same conclusion is valid for all phases evaluated in this study.

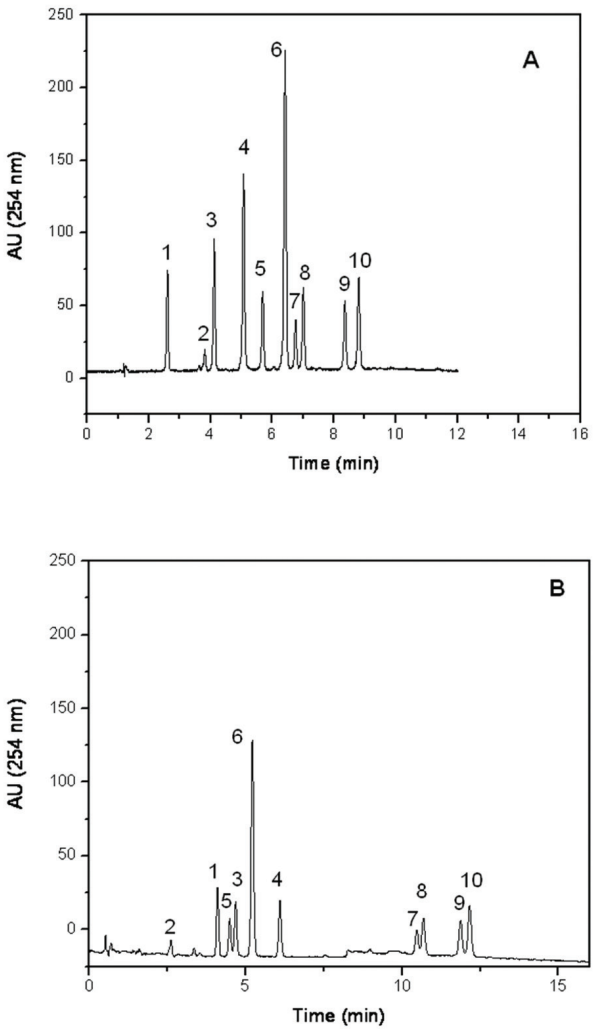

Figure 4. Chromatograms of the 10-component test mixture on the 1,2,4-triazole column (15 cm x 4.6 mm i.d., 5 µm d_p) and the *click* Phenol column (15 cm x 3 mm i.d., 5 µm d_p (B). The separation conditions were as follows: (A) Flow rate CO_2 2.0 mL/min, flow rate modifier from 0-20 min 0.12 to 1.0 mL/min (5.7 – 33% modifier). (B) Flow rate CO_2 = 1.6 mL/min, flow rate modifier from 0-20 min 0.1 to 0.8 mL/min (5.7 – 33% modifier). Modifier MeOH 20 mM ammoniumformate. Detection UV 254 nm. Temperature 40°C. Peaks: 1. caffeine, 2. ibuprofen, 3. theophylline, 4. theobromine, 5. fenoprofen, 6. flurbiprofen, 7. cortisone, 8. prednisone, 9. hydrocortisone, 10. prednisolone.

The C-Phe column was selected for the analysis of metoclopramide and its potential impurities by SFC-TOFMS operated in the positive APCI mode. Details on

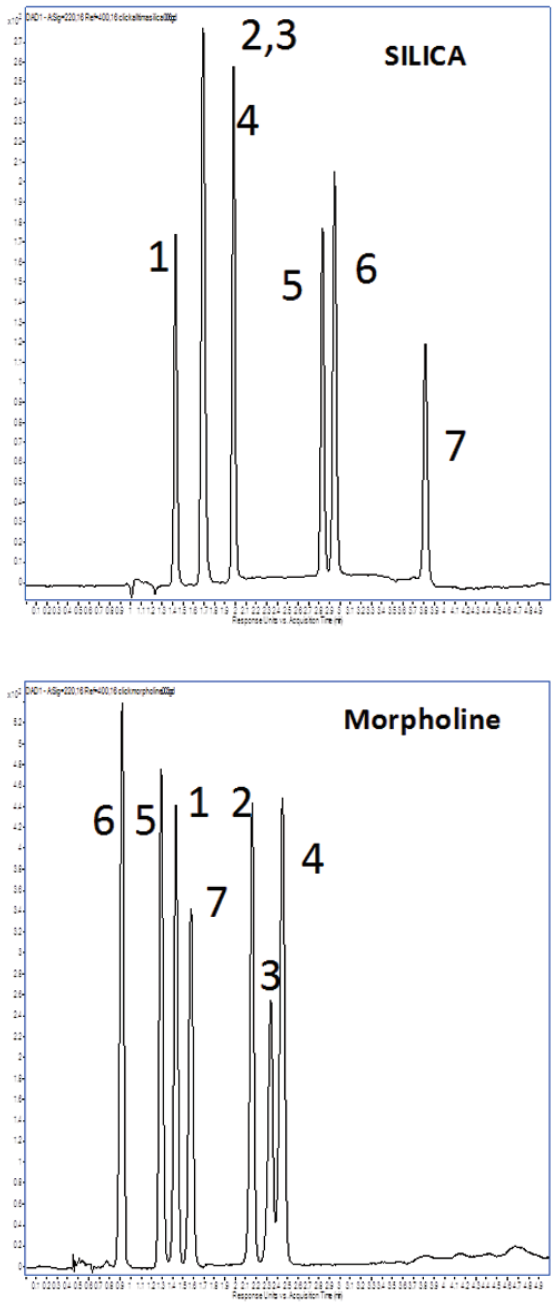

Figure 5. Chromatograms of the acid-base mixture on (A) bare silica (15 cm x 4.6 mm i.d., 3 µm d_p) and (B) *click* Morpholine (15 cm x 3 mm i.d., 5 µm d_p). The separation conditions were as follows: Flow rate CO_2 2.0 mL/min, flow rate modifier from 0-5 min 0.2 to 0.7 mL/min. Modifier MeOH. Detection = UV 254 nm. Temperature = 40°C. Peaks: 1. ibuprofen, 2. flurbiprofen, 3. fenoprofen, 4. ketoprofen, 5. theophylline, 6. caffeine, 7. theophyllinfe.

the coupling can be found in ref[20,21]. Metoclopramide is basic (pK_a 9.3), and the impurities contain a mixture of acidic and basic compounds (Table 4). To enhance ionization 20 mM ammonium formate was added to the mobile phases. Figure 6 shows the UV and MS trace for the active pharmaceutical ingredient with the impurities

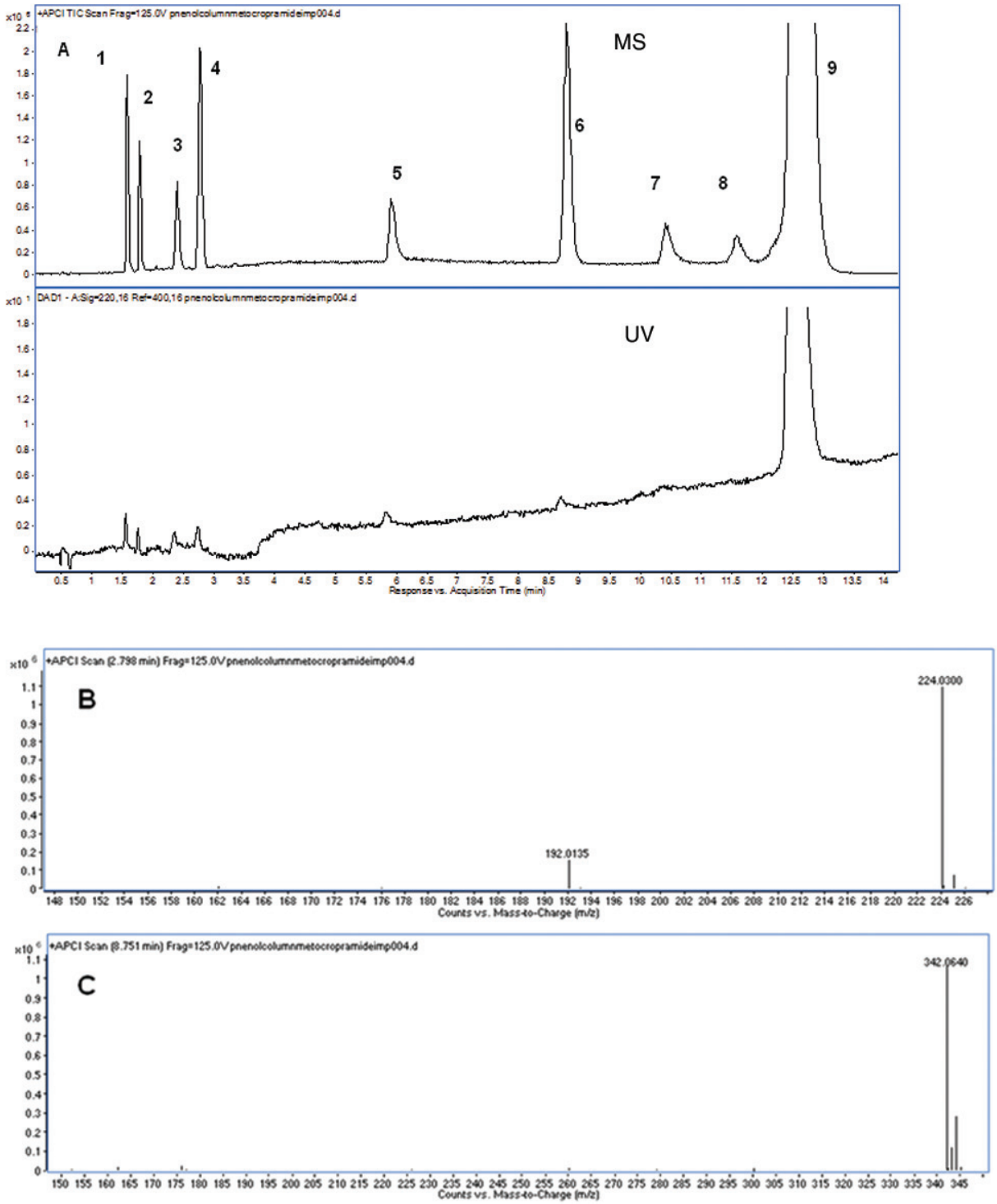

Figure 6. SFC-UV-TOFMS (A) of Metoclopramide and impurities at 0.02% level. Column: *click* Phenol column (15 cm x 3 mm i.d., 5 µm d_p).Separation Conditions: flow rate CO_2 1.6 mL/min, flow rate modifier from 0-21 min 0.1 to 1.2 mL/min. Modifier MeOH with 20 mM NH_4OOCH. UV 220 nm. MS scan. Temperature = 40°C. Outlet pressure 100 bar (fixed restrictor[28]). Injection 5 µL (metoclopramide 5 mg/mL, impurities at 0.02%). Mass spectra of peak 4 (B) and 6(C).

Table 4. Metoclopramide and impurities.

Peak	Name	Structure
1	Methyl 4-(acetylamino)-5-chloro-2-methoxybenzoate	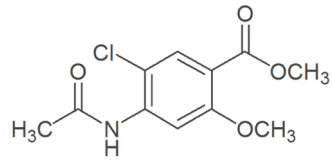
2	Methyl 4-amino-2-methoxybenzoate	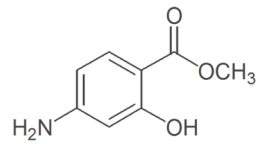
3	Methyl 4-(acetylamino)-2-hydroxybenzoate	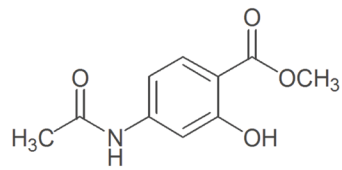
4	Methyl 4-(acetylamino)- 2-methoxybenzoate	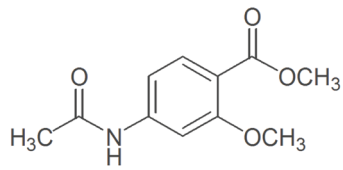
5	4-Amino-5-chloro-2-methoxybenzoic acid	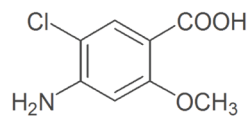
6	4-(Acetylamino)-5-chloro-N-2-(diethylaminoethyl)-2-methoxybenzamide	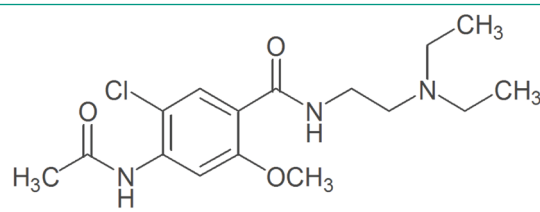
7	4-Amino-5-chloro-N-2-(diethylaminoethyl)-2-hydroxybenzamide	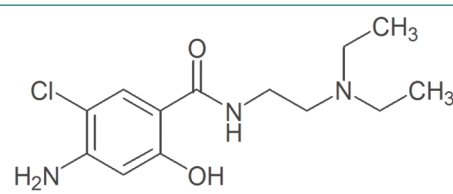
8	4-Amino-5-chloro-N-2-(diethylaminoethyl)-2-methoxybenzamide N-oxide	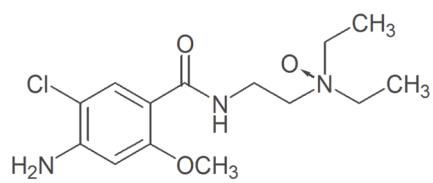
9	Metoclopramide	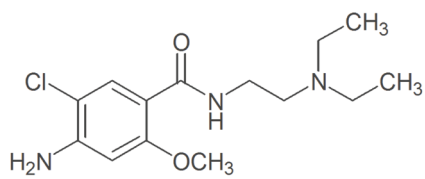

at the 0.02% level. In UV detection, only the 0.2% level could be quantified while the sensitivity in MS is much higher, easily allowing quantification at the 0.02% level. One of the advantages of SFC-APCI compared to reversed-phase LC-electrospray ionization (ESI) is that the spectra are very clean $[M+H]^+$ without formation of adducts typically observed in ESI. The mass spectra of impurity 4 and 6, both at 5 ng absolute on the column, are shown in Figure 6 C and D. Note also the excellent baseline in the scan SFC-MS trace illustrating that bleeding of the C-Phe is absent.

4. Conclusions

Stationary phases with different functionalities can easily be synthesized by the copper (I)-catalyzed azide-alkyne cycloaddition *click* reaction. Phenol, aniline, morpholine and pyridine were incorporated via a 1,2,3-triazole ring on aminopropyl silica. The C-Phe and C-Mor are complementary phases to the polar bare silica, 2-ethyl pyridine and 1,2,4-triazole. Based on the LSER studies, the main differences between the phases are related to the hydrogen-bonding capabilities (*a* and *b* coefficients), explaining the different elution orders observed between acidic and basic solutes. Additionally, it was shown that these *clicked* columns can be utilized for real-life applications. A pharmaceutical sample and impurities were analyzed using the C-Phe column with TOFMS detection in which 0.02% impurity levels were detected, which is sensitive enough for drug discovery.

Acknowledgements

We thank The Research Foundation – Flanders (FWO) for study grant G.0720.09N. The authors would also like to thank Mel Euerby of HiChrom for packing the *click* material into empty column hardware.

References

1. H. C. Kolb, M. G. Finn, K. B. Sharpless, Angew. Chem. Int. Ed. 40 (2001) 2004.
2. C. D. Hein, X.-M. Liu, D. Wang, Pharm. Res. 25, (2008) 2216.
3. H. C. Kolb, K. B. Sharpless, Drug Discov. Today 8 (2003) 1128.
4. M. Colombo, I. Peretto, Drug Discov. Today 13 (2008) 677.
5. K.M. Kacprzak, N.M. Maier, W. Lindner, Tetrahedron Lett. 47 (2006) 8721.
6. M. Slater, M. Snauko, F. Svec, J.M.J. Frechet, Anal. Chem. 78 (2006) 4969.
7. V.D. Bock, H. Hiemstra, J.H. van Maarseveen, Eur. J. Org. Chem.1 (2006) 51.
8. R. Huisgen, G. Szeimies, L. Mobius, Chem. Ber. 100 (1967) 2494.
9. F. Himo, T. Lovell, R. Hilgraf, V.V. Rostovtsev, L. Noodleman, K.B. Sharpless, V.V. Fokin, J. Am. Chem. Soc. 127 (2004) 210.
10. Z. Guo, A. Lei, X. Liang, Q. Xu, Chem. Commun. 43 (2006) 4512.
11. Z. Guo, A. Lei, Y. Zhang, Q. Xu, X. Xue, F. Zhang, X. Liang, Chem. Commun. 24 (2007) 2491.
12. G. Lei, X. Xiong, Y. Wei, X. Zheng, J. Zheng, J. Chromatogr. A 1187 (2008) 197.
13. Y. Zhang, Z. Guo, J. Ye, Q. Xu, X. Liang, A. Lei, J. Chromatogr. A 1191 (2008) 188.
14. S. E. Van der Plas, E. Van Hoeck, F. Lynen, P. Sandra, A. Madder, Eur. J. Org. Chem. 11 (2009) 1796.
15. E. Klesper, A.H. Corwin, D.A. Turner, J. Org. Chem. 27 (1962) 700.
16. T. Berger, C. Berger, R. Majors, LCGC North America, May 1, 2010.
17. C. West, E. Lesellier, J. Chromatogr. A 1191 (2008) 21.
18. C. West, E. Lesellier, J. Chromatogr. A 1203 (2008) 105.
19. C. West, E. Lesellier, in: E. Grushka, N. Grinberg (Eds.), Advances in Chromatography, Vol. 48, CRC Press, Boca Raton, FL, 2010, pp.195
20. P. Sandra, A. Pereira, M. Dunkle, C. Brunelli, F. David, LC.GC Europe, Volume 23 (2010) 396.
21. A. Pereira, F. David, G. Vanhoenacker, C. Brunelli, P. Sandra, LC.GC North America, Volume 29 (2011) 1006
22. M.F. Vitha, P.W. Carr, J. Chromatogr. A 1126 (2006) 143.
23. J. Verron, P. Malherbe, E. Prinssen, A.W. Thomas, N. Nock, R. Masciadri, Tetrahedron Lett. 48 (2007) 377.
24. J. Blake, C.H. Li, Proc. Natl. Acad. Sci. USA 78 (1981) 4055.
25. E.A. Crowell, C.S. Ough, A. Bakalinsky, Am. J. Enol. Vitic. 36 (1985) 175.
26. F.L. Lin, H.M. Hoyt, H. van Halbeek, R. G. Bergman, C. R. Bertozzi, J. Am. Chem. Soc. 127 (2005) 2686.
27. L.T. Taylor, M. Ashraf-Khorassani, LC.GC North America, 28 (2010) 810
28. T.A. Berger, J. Chromatogr. A, doi: 10.1016/j.chroma.2011.04.071